Metalurgi (2022) 3: 97 - 104

METALURGI
Majalah Ilmu dan Teknologi
p-ISSN 0126-3188 | e-ISSN 2443-3926
ejurnalmaterialmetalurgi.lipi.go.id

ANODIZING-ELECTRODEPOSITION HYBRID COATING BY USING SYNTHESIZED NATRIUM SILICATE AND ZIRCONIUM OXIDE ON THE SURFACE MAGNESIUM AZ31B

Aprilia Erryani[a], Bunga Rani Elvira[a], Syifa Ranggayoni Nurbaiti[b], Amalia Syahiddah[b], Hafsah Mujahidah[b], Yudi NugrahaThaha[a], Esmar Budi[b]

[a]Research Center for Metallurgy, National Research and Innovation Agency
Management Building 720, B.J. Habibie Sains and Technology Area, Banten, Indonesia 15314
[b]Fisika, Universitas Negeri Jakarta
Jl. R. Mangun Muka Raya No.11, Jakarta Timur, Indonesia
*E-mail: apri005@brin.go.id

Received: 02-10-2022, Revised: 08-11-2022, Accepted: 31-12-2022

Abstract

In this study, sodium silicate was synthesized, and zirconia was characterized as a suspension solution for anodization and electrodeposition processes. The results of the FTIR (fourier transform infrared) synthesis demonstrated the success of producing Na_2SiO_3 with the appearance of absorption from functional groups such as silanol (Si-OH) and siloxane (Si-O-Si) According to the SEM (scanning electron microscope) data, each batch contains oxygen, sodium, and silicon, indicating that Na_2SiO_3 was successfully synthesized without any detectable impurities. SEM images revealed that the calcination of $ZrOCl_2.8H_2O$ was dominated by zircon elements, with batch 3 having the highest zircon content at 88.81%. The XRD (x-ray diffraction) results show that ZrO_2 (monoclinic) dominates, with Cl_2 present in batches 1 and 3. As a result, the ZrO_2 used without calcination is in batch 3. Anodizing and electrodeposition processes can be performed in three ways: a. anodizing, b. two steps (anodizing-electrodeposition), and c. one step hybrid (anodizing and electrodeposition) with the addition of Al_2O_3 and $Na_2O_7SiO_3$ elements to the electrolyte. After coating, the surface of magnesium appears to be a pale white line. SEM images revealed that all three methods are coated and contain elements such as O, Na, Mg, Zr, Si, K, and Al in method c. The three samples also revealed that the sanding process was not optimal and that the Zr particles on the surface were not evenly distributed.

Keywords: *Anodizing, electrodeposition, ZrO_2, sodium silicate, magnesium*

1. INTRODUCTION

Biomaterials are materials that have direct contact with biological systems in living things, these materials are required to have several requirements, including not causing adverse effects on the body, having corrosion resistance, and having good strength [1]. In their application, biomaterials are used to replace or restore the function of bone components that have failed or been damaged. [2]. Several biomedical components such as artificial joints, implants, and drug delivery systems require the use of materials with biocompatible and biodegradable properties, thus requiring the development of new biomaterials that can be used for these applications [3]-[4]. In recent years, all attention has focused on biodegradable materials that serve to provide temporary support for fractures and will dissolve in the human body without harming their health [5].

Implants are a type of biomaterial used to replace bone tissue that has been damaged or is no longer functional as a result of disease or accident [6]. The term biodegradable on implants refers to the material's ability to corrode or degrade in the human body [7].

At present, magnesium metal (Mg) and its alloys are of concern because they are the right materials for implant applications that can be degraded in the body gradually, beneficial in

DOI : 10.14203/metalurgi.v37i3.680

Metalurgi is Sinta 2 Journal (https://sinta.ristekbrin.go.id/journals/detail?id=3708) accredited by Ministry of Research & Technology, Republic Indonesia

their absorption, if excessive levels can be excreted (excreted) through urine [8]-[11]. The release of Mg^{2+} ions into the body can help the growth of bone tissue and speed up healing time. Mg has good biocompatibility, low density, high specific strength, and a modulus of elasticity that is almost the same as a bone so that it can avoid stress shielding on bone [12]-[13].

Magnesium is the lightest metal that can be degraded through corrosion that occurs in body fluids [9]. However, its high solubility is also a weakness for magnesium, which can corrode rapidly in physiological pH (7.4-7.6) and high chloride physiological environment, so mechanical properties decrease before healing and new tissue growth [14]-[16].

Proper surface treatment can increase the wear and corrosion resistance of the substrate [17]. There are several surface treatment techniques developed to protect magnesium and its alloys. These techniques include chemical conversion coating, electrodeposition, anodizing, gas-phase deposition, organic coating, and sol-gel techniques [18].

The coating methods used in this research are anodizing and electrodeposition (electrodeposition). Anodizing can produce a passive film on the magnesium surface. The passive layer formed can reduce the corrosion rate of magnesium [19]. This method is very simple compared to other methods, so it reduced processing time. The coating results have a strong adhesion between the coating and the substrate, so it is good at controlling the corrosion rate of magnesium. [20].

In the electrodeposition process, charged particles or polymer macromolecules in suspension will move toward the electrode under the influence of an electric field [21]. The quality of the coating is determined by the length of time and the stress of the coating used. The longer the coating time, the thickness of the layer formed will increase [22]-[23].

An electrolyte solution containing a mixture of chemical compounds is required to carry out the anodizing and electrodeposition processes. The chemical compound $ZrOCl_2.8H_2O$ was calcined and silica was synthesized in this study. Zirconia can improve osteointegration and inhibit bacterial growth on the implant surface [24]. The calcination and synthesis processes were repeated three times in this study to determine suitable variables in the anodizing and electrodeposition processes. This research can prove that the synthesis of Na_2SiO_3 and the calcination of ZrO_2 can be used as a coating on magnesium through anodizing and electrodeposition processes. As a result, the purpose of this study was to investigate the effect of chemical compounds in suspension solution on magnesium coating using the electrodeposition method. The electrolyte solution and ZrO_2 electrodeposition coating process is expected to reduce corrosion while inhibiting the formation of a bacterial layer on the implant surface.

2. MATERIALS AND METHODS

2.1 Material Preparation

Magnesium AZ31B is the material used in this study. The following step is to make Na_2SiO_3 by dissolving 16 gr of NaOH in 100 ml of distilled water. A hotplate at 100 °C was used to heat 82.5 ml of the solution with 10 g of silica until crystals formed. Table 1 shows that the synthesis was performed three different times. Following that, all samples were heated for 30 minutes in a 500 °C furnace.

Table 1. Time in the synthesis process

Sample	Time (minute)
Bacth 1	120
Bacth 2	40
Bacth 3	25

Three experiments conditions for zircon calcination were carried out, as shown in Table 2.

Table 2. Content in the calcination zircon

Sample	Zircon (g)	Citric Acid (g)
Batch 1	3	1
Bacth 2	3	0.5
Bacth 3	3	0

To form a sol-gel, all materials were dissolved in 50 ml of distilled water in batches 1 and 2. After all the samples were ready, they were heated for 90 minutes in a muffle furnace at 200 °C and then for 3 hours in a muffle furnace at 700 °C.

Table 3. Suspended electrolytic for batch 1

Process	Contents
Anodizing	20 g Na_2SiO_3 3 g ZrO_2 7 g NaOH 7 g KF 7 g NaF

Following the calcination and synthesis processes, the results can be used as an electrolyte solution. To begin anodizing and electrodeposition, a suspended electrolyte is prepared.

Table 4. Suspended electrolytic for batch 2

Process	Contents
Anodizing	20 g Na_2SiO_3
	3 g ZrO_2
	7 g NaOH
	7 g KF
	7 g NaF
Electrodeposition	0.5 g Al_2O_3
	0,2 g Na_2HPO_4

The materials used to make the electrolyte solution are listed in Tables 3, 4, and 5. For both processes, all ingredients are dissolved in 500 mL of distilled water.

Table 5. Suspended electrolytic for batch 3

Process	Contents
Anodizing	20 g Na_2SiO_3
	3 g ZrO_2
	7 g NaOH
	7 g KF
	7 g NaF
Electrodeposition	0.5 g Al_2O_3
	0,25 g Na_2HPO_4
	0.5 g $Na_2O_7SO_3$

The anodization and electrodeposition process begins with two platinum anodes facing each other and a magnesium cathode. The three experiments were completed in 30 minutes using a rectifier.

2.1 SEM (Scanning Electron Microscope)

The surface topography and structural defects of the composite structure are examined using a SEM (scanning electron microscope). The SEM is a JEOL JSM6390A model. To determine the distribution of ZrO_2 in composites, SEM is supplemented by EDS (energy dispersive spectroscopy). Before testing, composite samples were coated with suspension.

2.2 FTIR (Fourier Transform Infrared)

The infrared absorption or emission spectra of solid, liquid, or gaseous substances can be obtained using the FTIR (fourier transform infrared) technique. FTIR's basic operation is to identify compounds, detect functional groups, and analyze desired mixtures and samples. In general, FTIR is frequently used to quantitatively and qualitatively identify organic compounds. FTIR is used in quantitative research to determine the concentration of analytes in a sample. FTIR was performed by Bruker in the wavenumber range 4000-350 cm^{-1} to identify the presence of functional groups on the sample with spectra resolution of 4 cm^{-1}, 45 scans, and Blackman-Harris 3-Term apodization.

2.3 XRD (X-Ray Diffraction)

XRD (x-ray diffraction) is used for material characterization and quality control of crystalline or non-crystalline materials such as powders, solid blocks, thin films or liquids. XRD is also used to determine composition and determine elements. From the XRD results it will be known which structure is formed. The working principle of the XRD tool is to use x-ray crystals which will then appear in a material to see the structure of the material. XRD test was performed by Smartlab Rigaku, carried out at 2θ from 20° to 90°. XRD measurements were operated at 15 mA and 40 kV using Cu Kα radiation.

3. RESULT AND DISCUSSION

3.1 Analysis Results SEM of Synthesis Na_2SiO_3

The synthesis of Na_2SiO_3 from SiO_2 can be seen from the SEM (scanning electron microscope) and EDS (energy dispersive spectrometry) images. The difference in heating time in the sol-gel process did not significantly affect the composition of Na_2SiO_3. The difference is seen in the shape of the crystals.

In batch 1 (Fig. 1(a)) the crystal form is the most lumpy and coarser. This is caused by unstable heating, making the process take a long time. In batch 2 (Fig. 2(b)), the crystal form is relatively finer than batch 1, however, the surface looks more porous than batch 2. In batch 3 (Fig. 3(c)), the crystal form is relatively cleaner and smoother than the two previous batches. This is because the heating is done at the right time and gets a good texture. The test results in all batches showed the detected water content. That's because, the nature of Na_2SiO_3 which is hygroscopic.

The results of qualitative analysis using EDS (Table 6) showed that pure sodium silicate was successfully synthesized in this experiment. This is indicated by the absence of impurities in the form of C or carbon atoms and impurity metals in all batches. It also shows that the length of time and temperature in the heating process did not affect the success of the synthesis. But it affects the shape of the synthesized crystal. When NaOH melts at high temperatures, it completely

dissociates to form Na+ ions and OH- ions. The high electronegativity of the O atom in SiO2 makes more Si electropositive, resulting in the formation of an unstable $[SiO_2OH]^-$ intermediate and dehydrogenation.

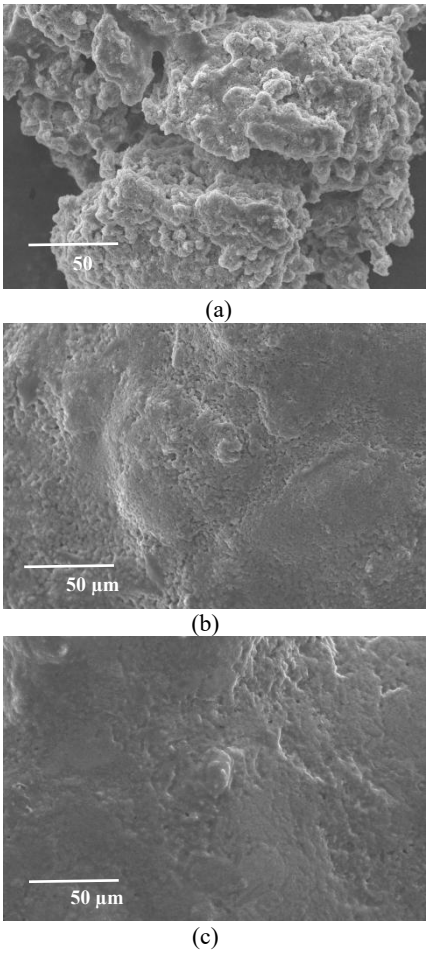

Figure 1. SEM images of Na_2SiO_3 synthesis at (a) Batch 1, (b) Batch 2, and (c) Batch 3

Melting at 500 °C is based on the melting point of NaOH, which is 318 °C, at which point NaOH completely dissociates to form Na^+ and OH^- ions. NaOH was chosen because it has a lower melting point than Na_2SiO_3 around 851 °C, allowing for the formation of sodium silicate at lower temperatures [25].

Tabel 6. EDS of synthesized Na_2SiO_3

		Batch 1	Batch 2	Batch 3
Element		Mass%	Mass%	Mass%
O	K	51.8177	50.6603	58.1238
Na	K	33.6874	36.8691	29.7613
Si	K	14.4949	12.4506	12.1149

The second OH^- ion will form a water molecule by bonding with hydrogen, and two Na^+ ions will balance the negative charge of SiO_3^{2-} ions to form sodium silicate [26].

The EDS data obtained revealed differences in the content of each sample, with batch 1 containing 37.14% O elements, 40.35% Na elements, and 22.50% Si elements. In batch 2, the EDS results contain 38.70% O elements, 44.87% Na elements, and 16.42% Si elements. Batch 3 contains 50.51% element O, 34.69% Na, and 12.79% Si.

3.2 Analysis Results FTIR of Synthesis Na_2SiO_3

The results of the analysis of sodium silicate with FTIR are shown in peaks chart. The results of the FTIR test on 3 batches did not show a significant difference in the wave pattern. The analysis of the FTIR results was carried out by characterizing the wave number range of 500-3500 cm^{-1} to determine the functional group of the main peak.

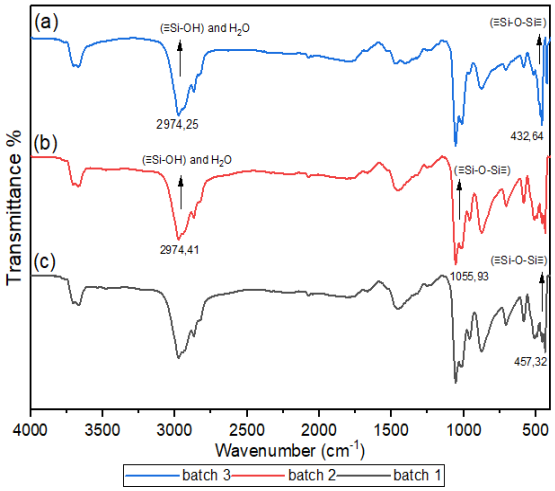

Figure 2. FTIR test results for Na_2SiO_3 synthesis at (a) Batch 3, (b) Batch 2, and (c) Batch 1

Silica absorption patterns that appear generally are silanol (≡Si-OH) and siloxane (≡Si-O-Si≡) groups. The absorption pattern obtained has a pattern that is quite similar to the results of research on the synthesis of Na_2SiO_3 conducted by Linda where the absorption band results obtained at wave numbers 432.64 cm^{-1}, and 457.32 cm^{-1} shows the bending vibration of the siloxane group (≡Si-O-Si≡). The absorption band at wavenumber at 1055.93 cm^{-1} show the Si-O asymmetric stretch vibration of siloxane (≡Si-O-Si≡), and the absorption band at wavenumber at 2974.25 cm^{-1}, and 2974.41 cm^{-1} indicates the -OH group of silanol (≡Si-OH) and H_2O [25].

The FTIR results show that SiO_2 is formed. The reaction that occurs for the formation of SiO2 is as follows:

$$C, H, \text{and } Si + 3O_2 \rightarrow CO_2(g) + 2H_2O(g) + SiO_2(s)$$

as well as a condensation of silanol groups (≡Si-OH) such as:

$$2\equiv Si\text{-}OH \equiv Si\text{-}O\text{-}Si \equiv + H_2O \text{ [27]}$$

Variations in heating time had no effect on the synthesis of Na_2SiO_3. As shown in Fig. 2, the absorption peak of the synthesized Na_2SiO_3 is relatively constant across all time variations.

3.3 Analysis Results SEM of Calcination ZrO_2

Figure 3 shows the SEM (scanning electron microscope) images from ZrO_2 calcination.

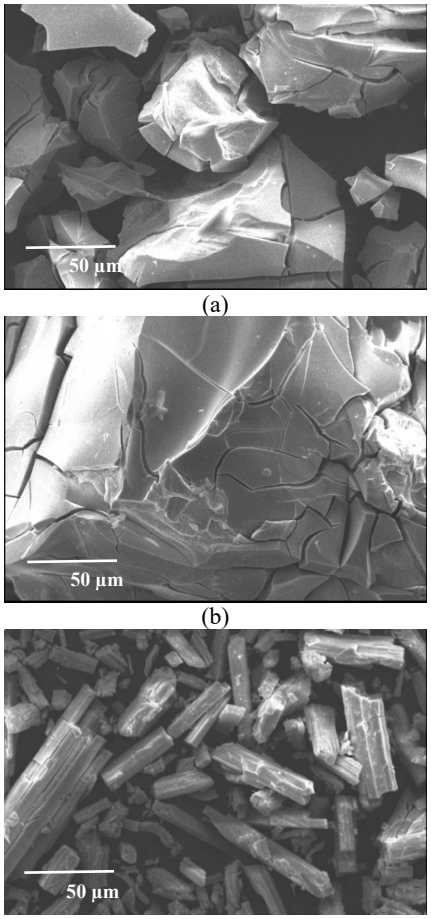

Figure 3. SEM results of ZrO_2 synthesis at (a) Batch 1, (b) Batch 2, and (c) Batch 3

In Figures 3(a) and 3(b), the solid crystal form is almost identical, which is like a lump.

Tabel 7. EDS of synthesized ZrO_2

		Batch 1	Batch 2	Batch 3
Element		Mass%	Mass%	Mass%
O	K	14.3314	56.4202	11.1863
Zr	L	85.6686	43.5798	88.8137

In contrast to Fig. 3(c), where only $ZrOCl_2.8H_2O$ is seen in the form of crystals-like chunks that are longer and scattered. According to the results of the EDS test, there were no impurities in the three batches tested, and the ZrO_2 had been calcined.

The ZrO_2 calcination process from $ZrOCl_2.8H_2O$ was carried out with three different citric acid contents (can be seen in the method). The EDS results (Table 7) for each batch show a different amount of ZrO_2. Batch 2 produces the most oxide of ZrO_2 (56.42%). Batches 1 and 3 were only 14.33% and 11.18%, respectively. According to the EDS results, the optimal amount of citric acid used to produce better calcination of ZrO_2 is 0.5 gram for 3 grams of $ZrOCl_2.8.H_2O$. The EDS results are also supported by XRD data, which will be discussed in the following sub-chapter.

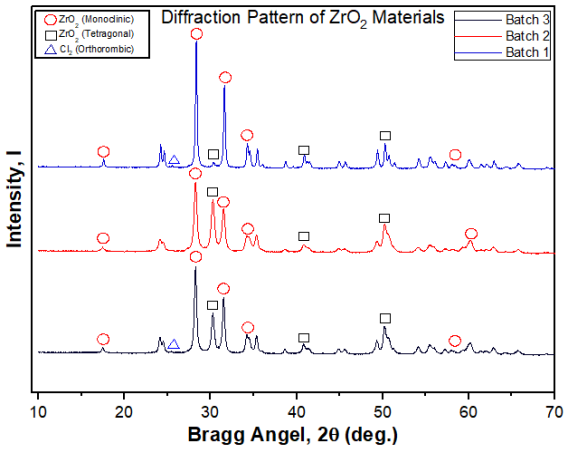

Figure 4. XRD pattern of syntesized ZrO_2

The ZrO_2 phase of the calcination results described previously in SEM images and EDS can be clarified using XRD measurements. Batches 1 and 3 of $ZrOCl_2.xH_2O$ calcination still left Cl_2. The presence of Cl_2 indicates that the calcination results of batches 1 and 3 are still incomplete due to the presence of Cl_2 impurities. There is no Cl_2 impurity in batch 2. Furthermore, ZrO_2 from batch 2 will be used in the Mg coating process.

3.5 Process Anodizing Electrodeposition Analysis Results

The hybrid coating process is accomplished through two methods, the first of which is accomplished in two stages (anodizing followed by electrodeposition). The second method, anodizing-electrodeposition, was carried out concurrently.

Figure 5(a) shows anodized magnesium AZ31B with a porous surface in several places; the striped structure is caused by the grounding process, which is not smooth and flat.

Magnesium AZ31B is well anodized, as shown in Fig. 5(a). The presence of elements O, Na, Mg, and Si was discovered using EDS data.

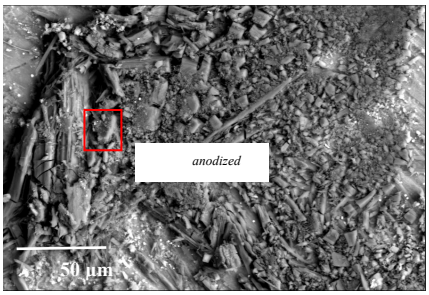

(a)

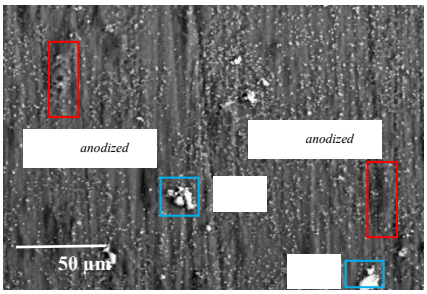

(b)

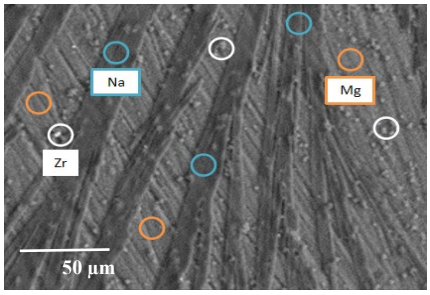

(c)

Figure 5. Photos of SEM results for the following processes; (a) Anodizing (b) Anodizing-electrodeposition in two step (c) Anodizing-electrodeposition hybrid

Following that, a two-stage coating process was carried out in which the surface of Magnesium AZ31B was anodized for 35 minutes to produce a porous structure. After Magnesium AZ31B had dried at room temperature, the process was resumed. The coating process was then continued for 35 minutes using the electrophoretic deposition method with ZrO_2. The dried product appears slightly blackened and pale whitish in color, indicating that it has been coated with Magnesium AZ31B.

Figure 5(b) shows anodized magnesium AZ31B. The ribbed structure is caused by the non-smooth and flat grounding process of Magnesium AZ31B. In several places, the surface is porous. Magnesium AZ31B is well anodized, as shown in Fig. 5(b), despite the fact that not many Zr particles are evenly distributed on the Mg surface during the electrodeposition process due to the large particle size of ZrO_2. ZrO_2 must be measured on a nanoscale to achieve optimal electrodeposition results [28].

In Figure 5(c), the coating was applied in a single step, with anodizing and electrophoretic deposition occurring concurrently for 30 minutes at a constant electric current of 1 A. Because of the rectifier used, the coating does not function as intended. The rectifier used has a maximum capacity of 15 volts and 1 amp current. The rectifier did not reach that number during the experiment using a variable volt with 5 volts, 10 volts, and 15 volts because the current generated was very large. Changing the variables into a suspension solution requires the addition of the chemical compounds $Na_2O_7SiO_3$ and Al_2O_3.

The coating process has an effect on the surface of Magnesium AZ31B when the dry color changes slightly to black and a pale white line appears. The surface of Magnesium AZ31B forms a porous layer in several places, indicating that it is well anodized, despite the fact that not many Zr particles are evenly distributed on the Mg surface during the electrodeposition process, as shown in Fig. 5(c). Many factors can contribute to this, including a coarse sanding process for Mg and zircon particles that are not yet nanoscale.

The two-stage coating process produces better results than the one-stage coating process. Figure 5(b) shows that the pores formed by the anodizing results and the ZrO2 attached to the magnesium surface are becoming more evenly distributed across the entire surface. When compared to a single-stage coating process, less adhering ZrO_2 occurs because fewer pores or oxide layers are formed (Fig. 5(c)).

Tabel 8. EDS of hybrid coating magnesium AZ31B

Element	Mass%
O k	14.9482
Na k	10.6089
Mg k	68.5592
Al k*	2.4567
Si k	1.707
K k	1.353
Zr k*	0.3647

The two-stage coating process achieves better results on the surface coating of Magnesium AZ31B. Oxide formed on the surface of the AZ31B magnesium substrate while forming a porous surface. With an oxidant layer and pores on the surface, ZrO_2

adheres more easily and is more evenly distributed on the surface during the electrodeposition process. According to the EDS results, several elements were detected on the surface of Magnesium AZ31B, which are listed in Table 6.

4. CONCLUSION

Using synthesized Na_2SiO_3 and ZrO_2, anodizing electrodeposition hybrid coating on the surface of Magnesium AZ31B was successfully completed. The synthesis of Na_2SiO_3 yielded nearly identical results in all three batches, with only the crystal form differing. This result indicated the presence of silanol and siloxane groups. Batch 2 calcination yields the best ZrO_2 calcination results in the absence of Cl_2 impurities.

The two-stage coating process outperforms the one-stage coating process. Because the two-stage coating process maximizes the formation of the oxide layer, ZrO_2 in the electrodeposition process adheres better and is more evenly distributed on the surface. However, producing ZrO_2 with a smaller size (nm scale) is required so that ZrO_2 can be more easily attached to the magnesium surface.

ACKNOWLEDGMENT

The author would like to thank the "National Research and Innovation Agency's Research Center for Metallurgy" for organizing this activity.

REFERENCES

[1] D. Bombac, M. Brojan, P. Fajfar, and F. Kosel, "Review of materials in medical applications", *RMZ-Materials and Geoenvironment.*, vol. 54, no. 4, pp. 471-499, 2007.

[2] O.O. Ige, L. E. Umoru, M. O. Adeoye, A. R. Adetunji, O. E. Olorunniwo, and I. I. Akomolafe, "Monitoring, control, and prevention practices of biomaterials corrosion-an overview", *Trends in Biomaterials Artificial Organs.*, vol. 23, pp. 93-104, 2009.

[3] S. V. Gohil, S. Suhail, J. Rose, T. Vella, and L. S. Nair, "Polymers and composites for orthopedic applications," *Journal of Materials and Devices for Bone Disorders,* chapter. 8, pp. 349-395, 2020.

[4] E. Göktürk and H. Erdal, "Biomedical applications of polyglycolic acid (PGA)," *Journal of Sakarya Üniversitesi Fen Bilimleri Enstitüsü Dergis,* vol. 21, no. 6, pp. 1237-1244, 2017. Doi: 10.16984/saufenbilder.283156.

[5] Nowosielski, R; Cesarz, K; Babilas, R. "Structure and corrosion properties of Mg70-xZn30Cax(x=0.4) alloys for biomedical applications." *Journal of Achievements in Materials and Manufacturing Engineering,* vol. 58, no. 1, pp. 7-15, 2013.

[6] G. Chandra, and A. Pandey, "Biodegradable bone implants in orthopedic applications: a review", *Biocybernetics and Biomedical Engineering*, vol. 40, pp. 596-610. 2020. Doi : 10.1016/j.bbe.2020.02.003.

[7] Y. F. Zheng, X. N. Gu, F. Witte, "Biodegradable metals." *Materials Science and Engineering Reports*, vol. 77, pp. 1-34, 2014. Doi : 10.1016/h. mser.2014.01.001.

[8] S. X. Zhang, C. Zhang, J. Zhao, J. Li, Y. X. Song, H. Tao, Y. Zhang, Y. Hey, Y. Jiang, and Y. Bian. "Research on an Mg-Zn Alloy as a degradable biomaterial." *Acta Biomaterialia*, vol. 6, no. 2, pp. 626-40, 2010. Doi:10.1016/j.actbio.2009.06.028.

[9] H. Waizy, J. M. Seits, R. Janin, "Biodegradable magnesium implants for orthopedic applications", *Journal of Materials Science.*, vol. 48, pp. 39-50, 2013.

[10] L. Chang, L. Tian, W. Liu, "Formation of dicalcium phosphate dihydrate on magnesium alloy by micro-arc oxidation coupled with hydrothermal treatment" *Corrosion Science*, vol. 72, pp. 118-124, 2013.

[11] P. Rosemann, and J. Schmidt, "Short and longterm degradation behavior of Mg-1Ca magnesium alloys and protective coatings based on plasma-chemical oxidation and biodegradable polymer coating in synthetic body fluid" *Materials and Corrosion*, vol. 64, no. 8, pp. 714-722, 2013.

[12] H. S. Brar, and B. P Jordan, "A study of a biodegradable Mg–3Sc–3Y alloy and the effect of self-passivation on the in vitro degradation" *Acta Biomaterialia*, vol. 9, no. 2, pp. 5331-5340, 2013.

[13] G. Song, "Control of biodegradation of biocompatable magnesium alloys," *Corrosion Science*, vol. 49, no. 4, pp. 1696-1701, 2007.

[14] F. Witte, V. Kaese, H. Haferkamp, E. Switzer, and A. M. Linderberg, C. J.

Wirth, H. Windhagen, “In vivo corrosion of four magnesium alloys and the associated bone response”, *Biomaterials*, vol. 26, pp. 3557-3563, 2005.

[15] C. E. Wen, M. Mabuchi, Y. Yamada, K. Shimojima, Y. Chino, “Processing of biocompatible porous Ti and Mg”, *Scripta Material*, vol. 45, pp.1147-53, 2001.

[16] M. B. T. Sofyan, O. Susanti, “Magnesium and its alloys as biomaterials: A literature review,” *Proceeding of Annual National Seminar on Mechanical Engineering XV*, 2016.

[17] G. B. Darband, M. Aliofkhazraei, PHamghalam, N. Valizade, “Plasma electrolytic oxidation of magnesium and its alloys: Mechanism, properties and applications”, *Journal of Magnesium and Alloys*, vol. 5, pp. 74-132, 2017.

[18] A. Galio, S. Lamaka, M. Zheludkevich, L. Dick, I. Müller, M. Ferreira, “Inhibitor-doped sol–gel coatings for corrosion protection of magnesium alloy AZ31”. *Surface & Coatings Technology*, vol. 204, pp. 1479-1486, 2010. Doi : 10.1016/j.surfcoat.2009.09.067.

[19] Yin Zheng-Zheng., Qi Wei-Chen. “Advances in coating on biodegradable magnesium alloys”. *Journal of Magnesium and Alloys*, vol. 8, pp. 42-65, 2020. Doi : 10.1016/j.jma.2019.09.008.

[20] J. Gayle and A. Mahapatro,” Magnesium based biodegradable metallic implant materials: Corrosion control and evaluation of surface coatings”, *Journal of Innovations in Corrosion and Materials Science,* vol. 9, pp. 3-27, 2019. Doi : 10.2174/2352094909666190228113315.

[21] Riszki, I. Trivina and Harmami, “The effect of temperature on the quality of coating type 304 stainless steel with chitosan by electrophoresis”, *Jurnal Sains dan Seni ITS*, vol. 4, no.1, pp. 2337-3520, 2015.

[22] I. K. Suarsana, “The effect of nickel plating time on copper in decorative chromium plating on the brightness level and layer thickness”, *Cakram: Scientific Journal of Mechanical Engineering*, vol. 2, pp. 48-60, 2008.

[23] Basmal, Bayuseno, S. Nugroho, ”Pengaruh suhu dan waktu pelapisan tembaga nikel pada baja karbon rendah secara electroplating terhadap nilai ketebalan dan kekasaran”, *Rotasi*, vol. 14, no. 2, pp. 23-28, 2013.

[24] F. H. Shünemann, M. E. G. Vinueza, R. Margini, M. Fredel, F. Silva, J. C. M. Souza, Y. Zhang, B. Henriques, “Zirconia surface modifications for implant dentistry”, *Journal of Materials Science & Engineering*, vol. 98, pp. 1294-1305, 2019. Doi : 10.1016/j.msec.2019.01.062.

[25] L. Trivana, S. Sugiarti, and E. Rohaeti, “Synthesis and characterization of sodium silicate (Na_2SiO_3) from rice husk”, *Journal of Environmental Science & Technology*, vol 7, no. 2, pp. 66-75, 2015.

[26] I. Nurhidayati, E. T. Wahyuni, H. A. Nurul, and R. H. Sarwendah, “Effect of stirring time on sodium silicate synthesis from mount kelud volcanic ash”, *Alchemy: Journal of Chemistry*, vol. 9, no. 2, pp. 48-53, 2021.

[27] Sriyanti, Taslimah, Nuryono, and Narsito, “Sintesis bahan hibrida amino-silika dari abu sekam padi melalui proses sol-gel”, *Jurnal Kimia Sains dan Aplikasi*, vol. 8, no. 1, pp. 1-8, 2005. Doi : 10.14710/jksa.8.1.1-8.

[28] R. Chaharmahali, A. Fattah-alhosseini, M. Nouri, and K. Babaei, “ Improving surface characteristics of PEO coatings of Mg and its alloys with zirconia nanoparticles: A review”, *Applied Surface Science Advances*, vol. 6, 100131, 2021. Doi : 10.1016/j.apsadv.2021.100131.